Atmos. Chem. Phys. Discuss., 9, 15541–15565, 2009
www.atmos-chem-phys-discuss.net/9/15541/2009/

Atmospheric Chemistry and Physics Discussions

This discussion paper is/has been under review for the journal *Atmospheric Chemistry and Physics (ACP)*. Please refer to the corresponding final paper in *ACP* if available.

Secondary organic material formed by methylglyoxal in aqueous aerosol mimics – Part 1: Surface tension depression and light-absorbing products

A. N. Schwier, E. L. Shapiro, N. Sareen, and V. F. McNeill

Department of Chemical Engineering, Columbia University, New York, NY, USA

Received: 15 July 2009 – Accepted: 18 July 2009 – Published: 24 July 2009

Correspondence to: V. F. McNeill (vfm2103@columbia.edu)

Published by Copernicus Publications on behalf of the European Geosciences Union.

Abstract

We show that methylglyoxal forms light-absorbing secondary organic material in aqueous ammonium sulfate and ammonium nitrate solutions mimicking tropospheric aerosol particles. The light-absorbing products form on the order of minutes, and solution composition continues to change over several days. The results suggest an aldol condensation pathway involving the participation of the ammonium ion. Aqueous solutions of methylglyoxal, with and without inorganic salts, exhibit surface tension depression. Methylglyoxal uptake could potentially change the optical properties, climate effects, and heterogeneous chemistry of the seed aerosol over its lifetime.

1 Introduction

Laboratory and field studies suggest that carbonyl-containing volatile organic compounds, when absorbed by aqueous aerosol particles or cloud droplets, participate in aqueous-phase chemistry to form low-volatility secondary organic material (SOA) (Jang et al., 2002; Kroll et al., 2005; Liggio et al., 2005a, b; Volkamer et al., 2006, 2007, 2009; Loeffler et al., 2006; Zhao et al., 2006; Gao et al., 2006; Altieri et al., 2008; Carlton et al., 2008; Nozière et al., 2009; Fu et al., 2009; Shapiro et al., 2009; Galloway et al., 2009; El Haddad et al., 2009; De Haan et al., 2009). There is evidence that SOA formation may affect properties of the seed aerosol such as CCN activity (Cruz and Pandis, 1997; Hartz et al., 2005; King et al., 2007, 2009; Englehardt et al., 2008; Duplissy et al., 2008; Michaud, et al., 2009) optical properties (Saathoff et al., 2003; Nozière et al., 2007, 2009; Nozière and Esteve, 2007; Casale et al., 2007; Shapiro et al., 2009; De Haan, et al., 2009) and heterogeneous reactivity towards gases such as N_2O_5 (Folkers et al., 2003; Anttila et al., 2006). A variety of potentially surface-active SOA products have been proposed, including organic acids, organosulfates, nitrogen-containing organics, aldol condensation products, and highly oxygenated oligomeric material. In an aqueous aerosol particle, surface-active products may partition to the

gas-particle interface, lowering the surface tension (and thus the critical supersaturation required for cloud droplet activation) and acting as a barrier to mass transport between the gas and aqueous phases. Light-absorbing SOA products which could increase the absorption index of the seed aerosol have also been identified in laboratory studies. Aldehydes have been reported to undergo aldol condensation in aqueous aerosol mimics to form π-conjugated species (Nozière et al., 2007; Nozière and Esteve, 2007; Casale et al., 2007). We recently reported the formation of light-absorbing, oligomeric molecules in aqueous aerosol mimics containing glyoxal and ammonium salts (Shapiro et al., 2009). De Haan et al. (2009) observed browning upon the reaction of glyoxal with amino acids in aerosol and cloud droplet mimics.

Methylglyoxal is an atmospheric oxidation product of many anthropogenic and biogenic volatile organic compounds (Tuazon et al., 1986; Grosjean et al., 1993; Smith et al., 1999). Methylglyoxal becomes hydrated and forms acetal and hemiacetal oligomers in aqueous solution (Nemet et al., 2004; Paulsen et al., 2005; Loeffler et al., 2006; Zhao et al., 2006; Krizner et al., 2009). Kalberer et al. (2004) suggested that methylglyoxal acetal oligomers could explain their observation of polymeric material in secondary organic aerosols formed in a reaction chamber by the photooxidation of 1,3,5-trimethylbenzene. Barsanti and Pankow (2005) and Krizner et al. (2009) predicted that aldol condensation should be favorable for methylglyoxal in aerosols. However, Kroll et al. (2005) observed no particle growth upon exposing acidic ammonium sulfate seed aerosols to gas-phase methylglyoxal in an aerosol chamber, in contrast with glyoxal, which caused significant particle growth under similar conditions.

We report that methylglyoxal forms light-absorbing secondary organic products in aqueous ammonium salt solutions mimicking tropospheric aerosol particles. Product formation has been characterized using UV-Vis spectrophotometry and by aerosol chemical ionization mass spectrometry, reported in a companion paper (Sareen et al., 2009). Pendant drop tensiometry measurements show that aqueous solutions of methylglyoxal exhibit surface tension depression, and the effect is enhanced when NaCl or $(NH_4)_2SO_4$ is present. These observations add to the growing body of ev-

idence that secondary organic aerosol formation via heterogeneous processes may affect seed aerosol properties.

2 Methods

Solutions were prepared using Millipore water and high concentrations of the salt of interest (3.1 M $(NH_4)_2SO_4$, 5.1 M NaCl, 1.18 M Na_2SO_4, 8.7 M NH_4NO_3), in order to mimic the composition of an aqueous atmospheric aerosol particle (Tang and Munkelwitz, 1994; Tang et al., 1997). Methylglyoxal concentrations ranged from 0–2.0 M, corresponding to ~0–25 wt% of the solute. Methylglyoxal was introduced from a 40 wt% aqueous solution (Sigma Aldrich). Mixing time was counted as time after the 40 wt% methylglyoxal solution was introduced to the aqueous salt solution. The aqueous methylglyoxal stock solution was pH=2(±1) when tested with pH paper, and the reaction mixtures were pH=2(±1), without buffering or further addition of acid. This is within the range of pH relevant to tropospheric aerosols (Keene et al., 2004; Zhang et al., 2007). Solutions were prepared in 100 mL Pyrex volumetric flasks. Pyrex is opaque to light with wavelengths <280 nm (Corning, Inc.), but the samples were not further protected from ambient light except for control experiments as specified in the text. All experiments were performed at ambient temperature and pressure.

The UV-Vis absorption spectra of the reaction mixtures were measured using an HP 8453 UV-Visible Spectrophotometer with a 10 mm open-top quartz cuvette.

Surface tension was measured using pendant drop tensiometry as described in Shapiro et al. (2009). Briefly, droplets of sample solution were suspended from the tip of a glass capillary tube using a 100 µL syringe mounted inside a chamber with quartz windows. Images were captured as described by Anastasiadis et al. (1987). The method of Canny (1986) was implemented in MATLAB 7.0 (The MathWorks, Inc.) for edge detection. Surface tension was calculated according to:

$$\sigma = \frac{\Delta\rho g d_e^2}{H} \quad (1)$$

where σ is surface tension, $\Delta\rho$ is the difference in density between the solution and the gas phase, d_e is the equatorial diameter of the droplet, and H is the shape factor (Adamson and Gast, 1997). The method of several selected planes was used for determining H based on the diameter of the drop at five intervals along the drop axis (Juza, 1997). Solution density was measured using an analytical balance readable to within ±10 µg (Denver Instruments).

Geometry optimizations and energy calculations were performed using Jaguar 6.0 (Schrodinger, Inc.) with the ChemBio3D interface (CambridgeSoft) in order to evaluate the UV-Vis absorption of potential products and the energetics of reaction pathways. Density functional theory (DFT) with the B3LYP functional and the cc-pVTZ(-f) basis set (Kendall et al., 1992) was used to predict the HOMO-LUMO difference (and thus UV-Vis absorption wavelengths) of proposed products. For purposes of comparison with Krizner et al. (2009) some additional calculations were performed with the 6-311G** basis set and Poisson-Boltzmann solvation (water solvent, ε=80.37, probe radius=1.40 Å). The Gibbs free energy of solvated species was calculated using half the gas phase entropy following Krizner et al. (2009).

3 Results

Solutions containing ≥0.16 M methylglyoxal and $(NH_4)_2SO_4$ became visibly colored immediately after mixing and became progressively darker in color with time. The color varied noticeably with initial methylglyoxal concentration; solutions with higher initial concentrations of methylglyoxal were darker in color.

3.1 UV-Vis absorption

The products formed by methylglyoxal in aqueous solutions containing $(NH_4)_2SO_4$ or NH_4NO_3 absorb light at UV and visible wavelengths (ref. Figs. 1–3).

Methylglyoxal in aqueous solution has a broad absorbance peak at 290 nm at ambient temperatures (Nemet et al., 2004). A kinetics study of 1.62 mM methylglyoxal in 3.1 M $(NH_4)_2SO_4$(aq) (Fig. 1a) shows that after a delay of ∼1 h, peaks grow in at 213 nm and 286 nm with roughly exponential time dependence. Upon mixing of a solution of 1.62 M aqueous methylglyoxal and 3.1 M $(NH_4)_2SO_4$, absorbance initially increases across all wavelengths (Fig. 1b). After 1 h, the absorption spectrum is saturated for λ=360 nm, and the baseline at high wavelengths returns to <0.5 AU. With increasing time, the saturated region of the spectrum extends to longer wavelengths and the tail shows increasing absorption at high wavelengths (λ>500 nm). Significant absorption at 550 nm is exhibited at <1 h and after 12 h, with absorption at up to 700 nm developing within 2–3 d.

The effect of initial methylglyoxal concentration on the UV-Vis spectra of solutions containing 3.1 M $(NH_4)_2SO_4$ 24 h after mixing is shown in Fig. 2. As shown in Fig. 2b and c, the absorbance at 282 nm and at 550 nm at 24 h is linearly dependent on the initial methylglyoxal concentration. The results of several control experiments are shown in Fig. 3. Control samples containing 1.62 M methylglyoxal and 5.1 M NaCl or 1.18 M Na_2SO_4 exhibited UV-Vis spectra similar to aqueous methylglyoxal in the absence of salt after 24 h. A sample initially containing 1.62 M methylglyoxal and 3.1 M $(NH_4)_2SO_4$ was protected from light until analysis by covering the reaction vessel with aluminum foil, and the resulting spectrum at 24 h was identical to that of an unprotected solution with the same composition.

3.2 Surface tension

Solutions containing 3.1 M $(NH_4)_2SO_4$ and varying initial concentrations of methylglyoxal exhibit significant surface tension depression compared to 3.1 M $(NH_4)_2SO_4$ solutions without organics (Fig. 4). The surface tension depression follows a Langmuir-like dependence on initial methylglyoxal concentration, with a minimum (saturation) surface

tension, σ_{min}, of 41(±2) dyn cm^{-1} based on a fit to the data using the following equation:

$$\sigma = \sigma_0 - S\frac{bM_0}{1 + bM_0} \quad (2)$$

where σ is the surface tension, σ_0 is the surface tension of the solution with no methylglyoxal, M_0 is the initial methylglyoxal concentration, and S and b are fit parameters. Values of σ_0 for $(NH_4)_2SO_4$(aq) and NaCl(aq) were taken from the International Critical Tables (2003). The physical interpretation of S is the surface tension depression when the surface is saturated, such that $\sigma_{min}=\sigma_0-S$, and b is an equilibrium coefficient that describes surface-bulk partitioning. A time series was performed on a solution initially containing 1.62 M methylglyoxal and 3.1 M $(NH_4)_2SO_4$. The measured surface tension fluctuated for 2.5 h before stabilizing at 45(±1) dyn cm^{-1}, then slowly decreased over the next 21.5 h to the minimum value (41(±2) dyn cm^{-1}). Control experiments were performed in order to evaluate the role of $(NH_4)_2SO_4$. For aqueous methylglyoxal solutions with no salts present σ_{min}=52(±3) dyn cm^{-1}. Therefore, while hydrated methylglyoxal and/or the oligomers it forms in aqueous solution are surface-active, the overall surface-tension lowering effect is less than when $(NH_4)_2SO_4$ is present in solution. Solutions containing 5.1 M NaCl and varying amounts of methylglyoxal follow a trend similar to that of the $(NH_4)_2SO_4$ solutions, with σ_{min}=43(±2) dyn cm^{-1} (Fig. 4).

4 Discussion

The UV-Vis absorption data give evidence for reactions occurring on multiple timescales to produce at least two generations of products. Our observation that the UV-Vis spectrum of the methylglyoxal/$(NH_4)_2SO_4$ solution was the same at 24 h regardless of whether the solution was protected from light indicate that the reactions leading to light-absorbing compounds are not photochemical (Altieri et al., 2008). Our observation that methylglyoxal forms light-absorbing compounds when $(NH_4)_2SO_4$ or NH_4NO_3 was present, but not with NaCl and Na_2SO_4, suggests that NH_4^+ plays a role

in the mechanism. We propose that, in analogy to glyoxal, NH_4^+ participates via the formation of an iminium intermediate, or by acting as a Brønsted acid (Nozière et al., 2009; Galloway et al., 2009; Shapiro et al., 2009). The consequences of this could be a) the formation of species containing C-N bonds and b) facilitated oligomerization (acetal/hemiacetal formation and aldol condensation). Both C=N bonds and aldol condensation products may contribute to the observed absorbance in the visible. The calculations of Barsanti and Pankow (2005) and Krizner et al. (2009) suggest that aldol condensation should be favorable for methylglyoxal in aerosols, and it has long been known that methylglyoxal undergoes aldol condensation in the presence of amino acids to form brown products (Enders and Sigurdsson, 1943).

Singly hydrated methylglyoxal has been reported to be the dominant monomeric species in aqueous methylglyoxal systems (Nemet et al., 2004). Singly hydrated methylglyoxal may participate in self-aldol condensation via two possible pathways initiating with enol formation with the C=C double bond forming from either terminal carbon, as shown in Scheme 1. Note that we refer to the overall process of aldol addition followed by dehydration as aldol condensation (Muller, 1994).

Aldol addition via pathway (1) is likely to terminate in a dimer or trimer due to formation of organic acid or ketone end groups (e.g. species (c)–(g), Table 1). Additionally, because of the methyl group, many of the products of aldol addition via pathway (1) cannot proceed with dehydration (e.g. species (g), Table 1). Pathway (2) results in carbonyl termination (e.g. species (h) and (i), Table 1) and therefore aldol condensation could propagate beyond the trimer. The products would absorb at increasingly high wavelengths as the length of the conjugated polymer chain increases (Hudson and Kohler, 1974).

Krizner et al. (2009) showed that pathway (2) is thermodynamically favorable for aqueous methylglyoxal (they did not study pathway (1)). Our B3LYP/6-311G** calculations with Poisson-Boltzmann solvation show that ΔG=10.5 kcal mol^{-1} for the formation of the pathway (1) enol from singly hydrated methylglyoxal, close to Krizner et al.'s value of 11.9 kcal mol^{-1} for the formation of the pathway (2) enol, suggesting that both

enol species should be present in small quantities at equilibrium. Our calculations also show that the formation of a pathway (2) enol is more energetically favorable (ΔG=4.13 kcal mol^{-1}) than formation of the pathway (1) enol (ΔG=36.2 kcal mol^{-1}) for singly hydrated imine-substituted methylglyoxal (species (a), Table 1). This is consistent with NH_4^+ promoting pathway (2) over pathway (1), resulting in light-absorbing products. However, we anticipate that the concentration of imine-substituted species will be low due to the low NH_3 concentrations in our pH=2 solutions.

Referring to Fig. 1a, based on our B3LYP/cc-pvtz(-f) predictions, the species absorbing at 213 nm could correspond to an aldol addition product such as species (f) or (g) in Table 1. Acetals such as species (b) in Table 1 may also absorb at this wavelength. Aqueous methylglyoxal solutions with no salts present absorb at 290 nm, and this has been attributed to carbonyl-containing monomer and oligomer compounds (Nemet et al., 2004). Our observation of increasing absorbance at 286 nm with time indicates a shift in equilibrium towards species predicted to absorb near that wavelength, such as unhydrated methylglyoxal (B3LYP/ccptvz(-f) calculated λ=291.1 nm), or species (c), which is the aldol condensation product corresponding to species (f) (λ=271.1 nm). The pathway (2) aldol addition product species (h) is predicted to absorb at 320 nm.

The initial increase in baseline UV-Vis absorption upon mixing of aqueous methylglyoxal and $(NH_4)_2SO_4$ demonstrated in Fig. 1b indicates the fast formation of at least one light-absorbing reaction intermediate that is consumed in later steps of the mechanism (or as the equilibrium system recovers from the perturbation). Using the equilibrium constant data from Krizner et al. (2009), we predict that 99% of the methylglyoxal in aqueous solution is monomeric. Due to its fast formation it is expected that the absorbing intermediate is a first-generation product of a monomer species reacting with ammonium sulfate or with itself. Singly hydrated imine-substituted methylglyoxal (Table 1 species (a)), the expected reaction product between singly hydrated methylglyoxal and ammonium sulfate, is predicted to absorb at low wavelengths (183.5 nm). Therefore we infer that the intermediate is formed by the reaction of two monomeric species. This

reaction necessarily takes place in conjunction with the existing network of equilibrium reactions in aqueous methylglyoxal solution, thus complicating analysis of the kinetic data. We may make a crude estimate of the rate constant for this process using a simplified model as follows: The evolution of a dimer species P_1 with time, assuming no side reactions and an irreversible reaction, is given by

$$[P_1] = \frac{1}{2}\left[M_0 - \left(\frac{1}{M_0} + 2kt\right)^{-1}\right] \quad (3)$$

where M_0 is the initial monomer concentration (taken to be 1.62 M) and k is the rate constant. An upper bound for the rate constant for this process of $k \leq 2\ M^{-1}\ min^{-1}$ can be estimated by assuming that 90% of the monomer initially present in the solution is consumed to form the dimer product within 3 min. This upper bound value is roughly 40 times greater than the aldol addition rate constant estimated by Krizner et al. (2009).

The data in Fig. 2b and c demonstrate a linear dependence for the absorbance at 282 nm and 550 nm on initial methylglyoxal concentration 24 h after mixing. The absorbance at 550 nm also shows a linear dependence on time for t>12 h. Therefore the slow buildup of the product P_2 responsible for the increase in absorption at 550 nm at long times can be modeled by

$$[P_2] = k^{\mathrm{I}} M_o t \quad (4)$$

where k^{I} is the (pseudo-) first-order rate coefficient. A linear fit to the data in Fig. 2c or the data for t>12 h in the lower panel of Fig. 1b can yield k^{I} if the molar absorptivity of the species absorbing at 550 nm is known. Assuming that the absorbing species is at least a dimer, an upper bound for its concentration after 98 h is 0.81 M. Following Beer's law we then obtain a lower-bound estimate of the molar absorptivity at 550 nm of $\varepsilon \geq 3.68\ L\ mol^{-1} cm^{-1}$. Using this value and the slope from either fit we find an upper limit for the rate coefficient of the slow process, $k^{\mathrm{I}} \leq 8 \times 10^{-5}\ min^{-1}$.

Surface tension depression for methylglyoxal solutions containing 5.1 M NaCl or 3.1 M $(NH_4)_2SO_4$ is greater than that observed for aqueous methylglyoxal in the ab-

sence of salts. The observed enhancement in surface tension depression is likely to be a physical effect of the salts rather than an effect of especially surface-active products formed by a chemical reaction of methylglyoxal with the salts. High salt concentrations can result in a decreased critical micelle concentration due to charge screening, and thus cause enhanced film formation (Matijevic and Pethica, 1958; Li et al., 1998). Salts can also decrease the solubility of organics, commonly referred to as "salting out" (Setschenow, 1889), possibly resulting in surface film formation. Salts have commonly been observed to enhance the surface tension lowering effects of HULIS and organic diacids (Shulman et al., 1996; Kiss et al., 2005; Asa-Awuku et al., 2008).

Glyoxal was previously observed not to be surface-active in hydrated form or to form surface-active products in aqueous $(NH_4)_2SO_4$ solutions (Shapiro et al., 2009). Compared with glyoxal, the methyl group adds hydrophobicity to methylglyoxal and its oligomer products, increasing their surface activity.

5 Atmospheric implications

What we have observed for the methylglyoxal/$(NH_4)_2SO_4$ system is another example of aerosol-phase chemistry which may increase the absorption index of atmospheric aerosols with aerosol age. Following Nozière et al. (2009), the extinction coefficient at 550 nm for the solution initially containing 1.62 M methylglyoxal and 3.1 M $(NH_4)_2SO_4$ after 3 min is ε_{550}=2.11 cm^{-1} and the dimensionless absorption index, $A_{550}=\lambda\varepsilon_{550}/4\pi=9.23\times10^{-6}$. At 98 h, ε_{550}=2.98 cm^{-1} and $A_{550}=1.3\times10^{-5}$.

Our observation of surface tension depression is consistent with observations of surface tension depression by HULIS in ambient aerosol samples (Kiss et al., 2005; Salma et al., 2006; Taraniuk et al., 2007; Asa-Awuku et al., 2008). Decreased aerosol surface tension leads to a reduction in the critical supersaturation necessary for cloud droplet activation according to Kohler theory (Kohler, 1936). Surface tension depression in aqueous aerosols by methylglyoxal SOA material could therefore result in increased CCN activation. For particles of a given size, the effect of surface tension depression

on CCN activation can be expressed as:

$$s_c^* = \left(\frac{\sigma}{\sigma_w}\right)^{3/2} s_c \quad (5)$$

where s_c^* is the critical supersaturation, σ_w and σ are the surface tension of water and the particle, respectively, and s_c is the critical supersaturation for a particle with the surface tension of water. For sufficiently high methylglyoxal concentration we expect σ/σ_w=0.6 (see Fig. 4), in which case the critical supersaturation will be 46% that of a particle with $\sigma=\sigma_w$. Relative to an aqueous ammonium sulfate particle with no organics present, the critical supersaturation could be reduced by 62% at these methylglyoxal concentrations.

The small size, and thus high surface area-to-volume ratio of a submicron aerosol particle means that, compared to the bulk solutions used here, a greater fraction of the total surfactant molecules present in the aerosol will partition to the interface. This will raise the number of molecules that can be present before a full monolayer is formed and the critical micelle concentration (CMC) is reached (McNeill et al., 2006). Based on this effect, we would expect the minimum surface tension in an aerosol particle to be similar to what was observed here, but the plateau region of the surface tension curve may not be reached until higher methylglyoxal concentrations. However, this effect may be balanced by the fact that the small size of aerosol particles also leads to supersaturated salt concentrations which were not accessible in this study (Tang and Munkelwitz, 1994; Tang, 1997; Tang et al., 1997). The CMC lowering effect of the salt and the increased "salting-out" may counteract the size effect.

The atmospheric significance of the methylglyoxal heterogeneous SOA formation pathway will depend on the uptake of methylglyoxal from the gas phase into the aerosol. Like glyoxal, because of oligomer formation it is possible to achieve high concentrations of methylglyoxal in aqueous solution. However, the effective Henry's law coefficient for methylglyoxal in water has been reported to be orders of magnitude lower than that of glyoxal (Betterton and Hoffmann, 1988; Zhou and Mopper, 1990). The effective

Henry's law coefficient may increase when ammonium sulfate is present in the aqueous phase due to the aqueous-phase chemistry we have observed here. However, Kroll et al. (2005) reported negligible particle growth when ammonium sulfate particles were exposed to ~960 ppb of methylglyoxal in aerosol chamber experiments on a timescale of several hours. Surface film formation such as is suggested by our surface tension measurements, even at submonolayer coverages (i.e. concentrations below the CMC), can also inhibit the reactive uptake of gas-phase species into the aerosol (Folkers et al., 2003; Thornton and Abbatt, 2005; McNeill et al., 2006; Anttila et al., 2006; McNeill et al., 2007; Stemmler et al., 2008). Film formation upon uptake of methylglyoxal to the aerosol could result in suppressed VOC uptake (and therefore suppressed SOA formation and particle growth).

Acknowledgements. The authors gratefully acknowledge the Koberstein group for use of the pendant drop tensiometer and for helpful discussions. This work was funded by the NASA Tropospheric Chemistry program (grant NNX09AF26G) and by a Columbia University Professional Schools Research Fellowship for V.F.M. A.N.S. and E.L.S. contributed equally to this work.

References

Adamson, A. W. and Gast, A. P.: Physical chemistry of surfaces, Wiley, New York, 1997.

Altieri, K. E., Seitzinger, S. P., Carlton, A. G., Turpin, B. J., Klein, G. C., and Marshall, A. G.: Oligomers formed through in-cloud methylglyoxal reactions: Chemical composition, properties, and mechanisms investigated by ultra-high resolution FT-ICR mass spectrometry, Atmos. Environ., 42(7), 1476–1490, 2008.

Anastasiadis, S. H., Chen, J. K., Koberstein, J. T., Siegel, A. F., Sohn, J. E., and Emerson, J. A.: The Determination of Interfacial-Tension by Video Image-Processing of Pendant Fluid Drops, J. Colloid Interf. Sci., 119(1), 55–66, 1987.

Anttila, T., Kiendler-Scharr, A., Tillman, R., and Mentel, T. F.: On the Reactive Uptake of Gaseous Compounds by Organic-Coated Aqueous Aerosols: Theoretical Analysis and Application to the Heterogeneous Hydrolysis of N_2O_5, J. Phys. Chem. A, 110(35), 10435–10443, 2006.

Asa-Awuku, A., Sullivan, A. P., Hennigan, C. J., Weber, R. J., and Nenes, A.: Investigation of molar volume and surfactant characteristics of water-soluble organic compounds in biomass burning aerosol, Atmos. Chem. Phys., 8, 799–812, 2008, http://www.atmos-chem-phys.net/8/799/2008/.

Barsanti, K. C. and Pankow, J. F.: Thermodynamics of the formation of atmospheric organic particulate matter by accretion reactions – 2. Dialdehydes, methylglyoxal, and diketones, Atmos. Environ., 39(35), 6597–6607, 2005.

Betterton, E. A. and Hoffmann, M. R.: Henry Law Constants of Some Environmentally Important Aldehydes, Environ. Sci. Technol., 22(12), 1415–1418, 1988.

Canny, J.: A Computational Approach to Edge Detection, IEEE Trans. Patt. Anal. Mach. Intell., 8, 679–714, 1986.

Carlton, A. G., Turpin, B. J., Altieri, K. E., Seitzinger, S. P., Mathur, R., Roselle, S. J., and Weber, R. J.: CMAQ Model Performance Enhanced When In-Cloud Secondary Organic Aerosol is Included: Comparisons of Organic Carbon Predictions with Measurements, Environ. Sci. Technol., 42(23), 8798–8802, 2008.

Casale, M. T., Richman, A. R., Elrod, M. J., Garland, R. M., Beaver, M. R., and Tolbert, M. A.: Kinetics of acid-catalyzed aldol condensation reactions of aliphatic aldehydes, Atmos. Environ., 41(29), 6212–6224, 2007.

Cruz, C. N. and Pandis, S. N.: A study of the ability of pure secondary organic aerosol to act as cloud condensation nuclei, Atmos. Environ., 31(15), 2205–2214, 1997.

De Haan, D. O., Corrigan, A. L., Smith, K. W., Stroik, D. R., Turley, J. J., Lee, F. E., Tolbert, M. A., Jimenez, J. L., Cordova, K. E., and Ferrell, G. R.: Secondary Organic Aerosol-Forming Reactions of Glyoxal with Amino Acids, Environ. Sci. Technol., 43(8), 2818–2824, 2009.

Duplissy, J., Gysel, M., Alfarra, M. R., Dommen, J., Metzger, A., Prevot, A. S. H., Weingartner, E., Laaksonen, A., Raatikainen, T., Good, N., Turner, S. F., McFiggans, G., and Baltensperger, U.: Cloud forming potential of secondary organic aerosol under near atmospheric conditions, Geophys. Res. Lett., 35, L03818, doi:10.1029/2007GL031075, 2008.

El Haddad, I., Liu, Y., Nieto-Gligorovski, L., Michaud, V., Temime-Roussel, B., Quivet, E., Marchand, N., Sellegri, K., and Monod, A.: In-cloud processes of methacrolein under simulated conditions – Part 2: Formation of Secondary Organic Aerosol, Atmos. Chem. Phys. Discuss., 9, 6425–6449, 2009, http://www.atmos-chem-phys-discuss.net/9/6425/2009/.

Enders, C. and Sigurdsson, S.: The chemistry of humic acid formation under physiological

conditions, V. Announcement: The introductory phase of the humic acid formation. A aldol condensation from methylglyoxal, Ber. Dtsch. Chem. Ges., 76, 562–565, 1943.

Engelhart, G. J., Asa-Awuku, A., Nenes, A., and Pandis, S. N.: CCN activity and droplet growth kinetics of fresh and aged monoterpene secondary organic aerosol, Atmos. Chem. Phys., 8, 3937–3949, 2008, http://www.atmos-chem-phys.net/8/3937/2008/.

Folkers, M., Mentel, T. F., and Wahner, A.: Influence of an organic coating on the reactivity of aqueous aerosols probed by the heterogeneous hydrolysis of N_2O_5, Geophys. Res. Lett., 30(12), 1644–1647, 2003.

Fu, T. M., Jacob, D. J., and Heald, C. L.: Aqueous-phase reactive uptake of dicarbonyls as a source of organic aerosol over eastern North America, Atmos. Environ., 43(10), 1814–1822, 2009.

Galloway, M. M., Chhabra, P. S., Chan, A. W. H., Surratt, J. D., Flagan, R. C., Seinfeld, J. H., and Keutsch, F. N.: Glyoxal uptake on ammonium sulphate seed aerosol: reaction products and reversibility of uptake under dark and irradiated conditions, Atmos. Chem. Phys., 9, 3331–3345, 2009, http://www.atmos-chem-phys.net/9/3331/2009/.

Gao, S., Surratt, J. D., Knipping, E. M., Edgerton, E. S., Shahgholi, M., and Seinfeld, J. H.: Characterization of polar organic components in fine aerosols in the southeastern United States: Identity, origin, and evolution, J. Geophys. Res.-Atmos., 111(D14), D14314, doi:10.1029/2005JD006601, 2006.

Grosjean, D., Williams, E. L., and Grosjean, E.: Atmospheric Chemistry of Isoprene and of Its Carbonyl Products, Environ. Sci. Technol., 27(5), 830–840, 1993.

Hartz, K. E. H., Rosenoern, T., Ferchak, S. R., Raymond, T. M., Bilde, M., Donahue, N. M., and Pandis, S. N.: Cloud condensation nuclei activation of monoterpene and sesquiterpene secondary organic aerosol, J. Geophys. Res.-Atmos., 110(D14), D14208, doi:10.1029/2004JD005754, 2005.

Hudson, B. and Kohler, B.: Linear Polyene Electronic Structure and Spectroscopy, Ann. Rev. Phys. Chem., 25, 437–460, 1974.

International Critical Tables of Numerical Data, Physics, Chemistry, and Technology (1st Electronic Edition), edited by: Washburn, E. W., Knovel, Norwich, NY, 2003.

Jang, M. S., Czoschke, N. M., Lee, S., and Kamens, R. M.: Heterogeneous atmospheric aerosol production by acid-catalyzed particle-phase reactions, Science, 298(5594), 814–

817, 2002.

Juza, J.: The pendant drop method of surface tension measurement: Equation interpolating the shape factor tables for several selected planes, Czech. J. Phys., 47(3), 351–357, 1997.

Kalberer, M., Paulsen, D., Sax, M., Steinbacher, M., Dommen, J., Prevot, A. S. H., Fisseha, R., Weingartner, E., Frankevich, V., Zenobi, R., and Baltensperger, U.: Identification of polymers as major components of atmospheric organic aerosols, Science, 303(5664), 1659–1662, 2004.

Keene, W. C., Pszenny, A. A. P., Maben, J. R., Stevenson, E., and Wall, A.: Closure evaluation of size-resolved aerosol pH in the New England coastal atmosphere during summer, J. Geophys. Res.-Atmos., 109(D23), D23202, doi:10.1029/2004JD004801, 2004.

Kendall, R. A., Dunning, T. H., and Harrison, R. J.: Electron affinities of the first-row atoms revisited. Systematic basis sets and wave functions., J. Chem. Phys., 96(9), 6796–6806, 1992.

King, S. M., Rosenoern, T., Shilling, J. E., Chen, Q., and Martin, S. T.: Cloud condensation nucleus activity of secondary organic aerosol particles mixed with sulfate, Geophys. Res. Lett., 34(24), L24806, doi:10.1029/2007GL030390, 2007.

King, S. M., Rosenoern, T., Shilling, J. E., Chen, Q., and Martin, S. T.: Increased cloud activation potential of secondary organic aerosol for atmospheric mass loadings, Atmos. Chem. Phys., 9, 2959–2971, 2009, http://www.atmos-chem-phys.net/9/2959/2009/.

Kiss, G., Tombacz, E., and Hansson, H. C.: Surface tension effects of humic-like substances in the aqueous extract of tropospheric fine aerosol, J. Atmos. Chem., 50(3), 279–294, 2005.

Kohler, H.: The nucleus in the growth of hygroscopic droplets, Trans. Faraday Soc., 32, 1152–1161, 1936.

Krizner, H. E., De Haan, D. O., and Kua, J.: Thermodynamics and Kinetics of Methylglyoxal Dimer Formation: A Computational Study, J. Phys. Chem. A, 113(25), 6994–7001, 2009.

Kroll, J. H., Ng, N. L., Murphy, S. M., Varutbangkul, V., Flagan, R. C., and Seinfeld, J. H.: Chamber studies of secondary organic aerosol growth by reactive uptake of simple carbonyl compounds, J. Geophys. Res.-Atmos., 110(D23), D23207, doi:10.1029/2005JD006004, 2005.

Li, Z. D., Williams, A. L., and Rood, M. J.: Influence of soluble surfactant properties on the activation of aerosol particles containing inorganic solute, J. Atmos. Sci., 55(10), 1859–1866, 1998.

Liggio, J., Li, S. M., and McLaren, R.: Reactive uptake of glyoxal by particulate matter, J.

Geophys. Res.-Atmos., 110(D10), D10304, doi:10.1029/2004JD005113, 2005a.
Liggio, J., Li, S. M., and McLaren, R.: Heterogeneous reactions of glyoxal on particulate matter: Identification of acetals and sulfate esters, Environ. Sci. Technol., 39(6), 1532–1541, 2005b.
Loeffler, K. W., Koehler, C. A., Paul, N. M., and De Haan, D. O.: Oligomer formation in evaporating aqueous glyoxal and methyl glyoxal solutions, Environ. Sci. Technol., 40(20), 6318–6323, 2006.
Matijevic, E. and Pethica, B. A.: The properties of ionized monolayers, Part 1. Sodium dodecyl sulfate at the air/water interface, Trans. Faraday Soc., 54, 1383–1389, 1958.
McNeill, V. F., Wolfe, G. M., and Thornton, J. A.: The Oxidation of Oleate in Submicron Aqueous Salt Aerosols: Evidence of a Surface Process, J. Phys. Chem. A, 111, 1073–1083, 2007.
McNeill, V. F., Patterson, J., Wolfe, G. M., and Thornton, J. A.: The effect of varying levels of surfactant on the reactive uptake of N_2O_5 to aqueous aerosol, Atmos. Chem. Phys., 6, 1635–1644, 2006, http://www.atmos-chem-phys.net/6/1635/2006/.
Michaud, V., El Haddad, I., Liu, Y., Sellegri, K., Laj, P., Villani, P., Picard, D., Marchand, N., and Monod, A.: In-cloud processes of methacrolein under simulated conditions – Part 3: Hygroscopic and volatility properties of the formed Secondary Organic Aerosol, Atmos. Chem. Phys. Discuss., 9, 6451–6482, 2009, http://www.atmos-chem-phys-discuss.net/9/6451/2009/.
Muller, P.: Glossary of Terms Used in Physical Organic Chemistry (IUPAC Recommendations 1994), Pure Appl. Chem., 66(5) 1077–1184, 1994.
Nemet, I., Vikic-Topic, D., and Varga-Defterdarovic, L.: Spectroscopic studies of methylglyoxal in water and dimethylsulfoxide, Bioorg. Chem., 32(6), 560–570, 2004.
Nozière, B., Dziedzic, P., and Cordova, A.: Formation of secondary light-absorbing "fulvic-like" oligomers: A common process in aqueous and ionic atmospheric particles?, Geophys. Res. Lett., 34(21), L21812, doi:10.1029/2007GL031300, 2007.
Nozière, B., Dziedzic, P., and Cordova, A.: Products and Kinetics of the Liquid-Phase Reaction of Glyoxal Catalyzed by Ammonium Ions (NH_4^+), J. Phys. Chem. A, 113(1), 231–237, 2009.
Nozière, B. and Esteve, W.: Light-absorbing aldol condensation products in acidic aerosols: Spectra, kinetics, and contribution to the absorption index, Atmos. Environ., 41(6), 1150–1163, 2007.
Paulsen, D., Dommen, J., Kalberer, M., Prevot, A. S. H., Richter, R., Sax, M., Steinbacher, M., Weingartner, E., and Baltensperger, U.: Secondary organic aerosol formation by irradia-

tion of 1,3,5-trimethylbenzene-NO_x-H_2O in a new reaction chamber for Atmos. Chem. Phys., Environ. Sci. Technol., 39(8), 2668–2678, 2005.
Saathoff, H., Naumann, K. H., Schnaiter, M., Schock, W., Mohler, O., Schurath, U., Weingartner, E., Gysel, M., and Baltensperger, U.: Coating of soot and $(NH_4)_2SO_4$ particles by ozonolysis products of alpha-pinene, J. Aerosol Sci., 34(10), 1297–1321, 2003.
Salma, I., Ocskay, R., Varga, I., and Maenhaut, W.: Surface tension of atmospheric humic-like substances in connection with relaxation, dilution, and solution pH, J. Geophys. Res.-Atmos., 111(D23), D23205, doi:10.1029/2005JD007015, 2006.
Sareen, N., Shapiro, E. L., Schwier, A. N., and McNeill, V. F.: Secondary organic material formed by methylglyoxal in aqueous aerosol mimics – Part 2: Product identification using Aerosol-CIMS, Atmos. Chem. Phys. Discuss., 9, 15567–15594, 2009, http://www.atmos-chem-phys-discuss.net/9/15567/2009/.
Setschenow, J. Z.: Über die Konstitution der Salzlsungen auf Grund ihres Verhaltens zu Kohlensure, Z. Phys. Chem., 4, 117–125, 1889.
Shapiro, E. L., Szprengiel, J., Sareen, N., Jen, C. N., Giordano, M. R., and McNeill, V. F.: Light-absorbing secondary organic material formed by glyoxal in aqueous aerosol mimics, Atmos. Chem. Phys., 9, 2289–2300, 2009, http://www.atmos-chem-phys.net/9/2289/2009/.
Shulman, M. L., Jacobson, M. C., Carlson, R. J., Synovec, R. E., and Young, T. E.: Dissolution behavior and surface tension effects of organic compounds in nucleating cloud droplets, Geophys. Res. Lett., 23(3), 277–280, 1996.
Smith, D. F., Kleindienst, T. E., and Mciver, C. D.: Primary product distributions from the reaction of OH with *m*-, *p*-xylene, 1,2,4- and 1,3,5-trimethylbenzene, J. Atmos. Chem., 34(3), 339–364, 1999.
Stemmler, K., Vlasenko, A., Guimbaud, C., and Ammann, M.: The effect of fatty acid surfactants on the uptake of nitric acid to deliquesced NaCl aerosol, Atmos. Chem. Phys., 8, 5127–5141, 2008, http://www.atmos-chem-phys.net/8/5127/2008/.
Tang, I. N.: Thermodynamic and optical properties of mixed-salt aerosols of atmospheric importance, J. Geophys. Res.-Atmos., 102(D2), 1883–1893, 1997.
Tang, I. N. and Munkelwitz, H. R.: Water Activities, Densities, and Refractive-Indexes of Aqueous Sulfates and Sodium-Nitrate Droplets of Atmospheric Importance, J. Geophys. Res.-Atmos., 99(D9), 18801–18808, 1994.

Tang, I. N., Tridico, A. C., and Fung, K. H.: Thermodynamic and optical properties of sea salt aerosols, J. Geophys. Res.-Atmos., 102(D19), 23269–23275, 1997.

Taraniuk, I., Graber, E. R., Kostinski, A., and Rudich, Y.: Surfactant properties of atmospheric and model humic-like substances (HULIS), Geophys. Res. Lett., 34(16), L16807, doi:10.1029/2007GL029576, 2007.

Thornton, J. A. and Abbatt, J. P. D.: N_2O_5 Reaction on Sub-micron Sea Salt Aerosol: Effect of Surface Active Organics, J. Phys. Chem. A, 109(44), 10004–10012, 2005.

Tuazon, E. C., Macleod, H., Atkinson, R., and Carter, W. P. L.: Alpha-Dicarbonyl Yields from the NO_x-Air Photooxidations of A Series of Aromatic-Hydrocarbons in Air, Environ. Sci. Technol., 20(4), 383–387, 1986.

Volkamer, R., Jimenez, J. L., San Martini, F., Dzepina, K., Zhang, Q., Salcedo, D., Molina, L. T., Worsnop, D. R., and Molina, M. J.: Secondary organic aerosol formation from anthropogenic air pollution: Rapid and higher than expected, Geophys. Res. Lett., 33(17), L17811, doi:10.1029/2006GL026899, 2006.

Volkamer, R., San Martini, F., Molina, L. T., Salcedo, D., Jimenez, J. L., and Molina, M. J.: A missing sink for gas-phase glyoxal in Mexico City: Formation of secondary organic aerosol, Geophys. Res. Lett., 34, L19807, doi:10.1029/2007GL030752, 2007.

Volkamer, R., Ziemann, P. J., and Molina, M. J.: Secondary Organic Aerosol Formation from Acetylene (C_2H_2): seed effect on SOA yields due to organic photochemistry in the aerosol aqueous phase, Atmos. Chem. Phys., 9, 1907–1928, 2009, http://www.atmos-chem-phys.net/9/1907/2009/.

Zhang, Q., Jimenez, J. L., Worsnop, D. R., and Canagaratna, M.: A case study of urban particle acidity and its influence on secondary organic aerosol, Environ. Sci. Technol., 41(9), 3213–3219, 2007.

Zhao, J., Levitt, N. P., Zhang, R. Y., and Chen, J. M.: Heterogeneous reactions of methylglyoxal in acidic media: Implications for secondary organic aerosol formation, Environ. Sci. Technol., 40(24), 7682–7687, 2006.

Zhou, X. L. and Mopper, K.: Apparent Partition-Coefficients of 15 Carbonyl-Compounds Between Air and Seawater and Between Air and Fresh-Water – Implications for Air Sea Exchange, Environ. Sci. Technol., 24(12), 1864–1869, 1990.

Table 1. Proposed reaction products. Predictions for the energy of the gas phase HOMO-LUMO transition and the wavelength of UV-Vis absorption from DFT B3LYP/cc-pvtz(-f) simulations are shown. References are indicated by: 1) Nemet et al., 2004 2) Zhao et al., 2006 3) Krizner et al., 2009.

	Molecule	Ref.	energy (eV)	λ (nm)
a)		This work	6.757	183.5
b)	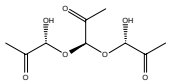	1,2	5.728	216.5
c)	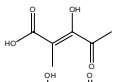	This work	4.574	271.1
d)	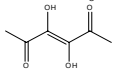	This work	3.536	350.6
e)	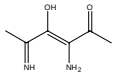	This work	3.354	369.6
f)	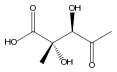	This work	6.247	198.5
g)	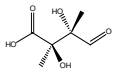	This work	5.751	215.6
h)	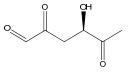	3	3.872	320.2
i)	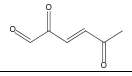	3	3.661	338.7

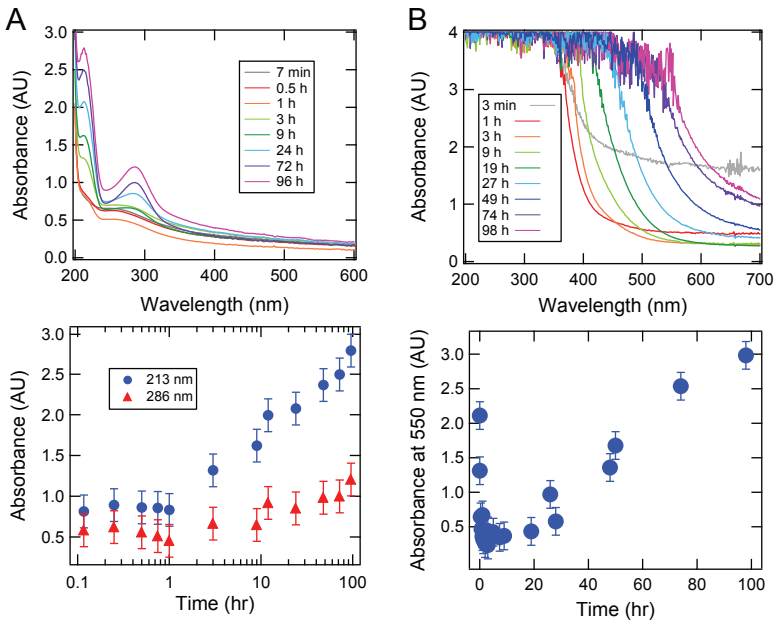

Fig. 1. UV-Vis spectra of aqueous solutions containing 3.1 M $(NH_4)_2SO_4$ and a) 1.62 mM methylglyoxal and b) 1.62 M methylglyoxal as a function of time after mixing. Absorbance is shown as a function of wavelength in the upper panels, and absorbance at selected wavelengths is shown in the lower panels. Error bars reflect uncertainty in the measured absorbances based on variation observed in the baseline signal.

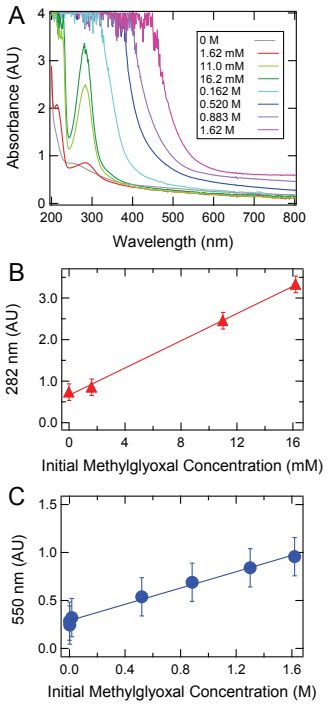

Fig. 2. UV-Vis spectra of aqueous solutions containing 3.1 M $(NH_4)_2SO_4$ and varying initial concentrations of methylglyoxal, 24 h after mixing. Absorbance is shown as a function of wavelength in panel **(a)**. Absorbance at 282 nm and 550 nm vs. initial methylglyoxal concentration are shown in panels **(b)** and **(c)**, respectively, along with linear least squares fits to the data. Error bars reflect uncertainty in the measured absorbances based on variation observed in the baseline signal.

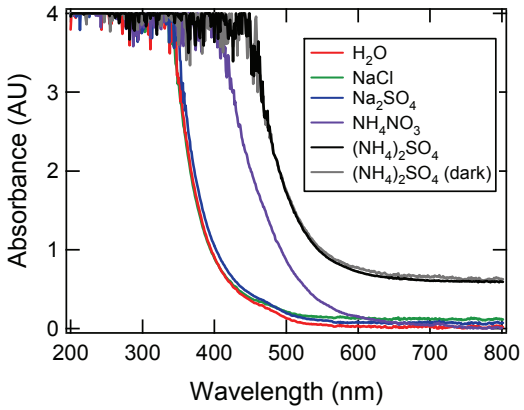

Fig. 3. UV-Vis spectra of control solutions. Absorbance is shown as a function of wavelength. Each aqueous solution initially contained 1.62 M methylglyoxal and: no salt, 5.1 M NaCl, 1.18 M Na_2SO_4, 8.7 M NH_4NO_3, or 3.1 M $(NH_4)_2SO_4$. Also shown is the spectrum of a solution initially containing 1.62 M methylglyoxal and 3.1 M $(NH_4)_2SO_4$ which was protected from light until analysis. All spectra were obtained 24 h after mixing, except for the NH_4NO_3 solution, which was measured at 96 h.

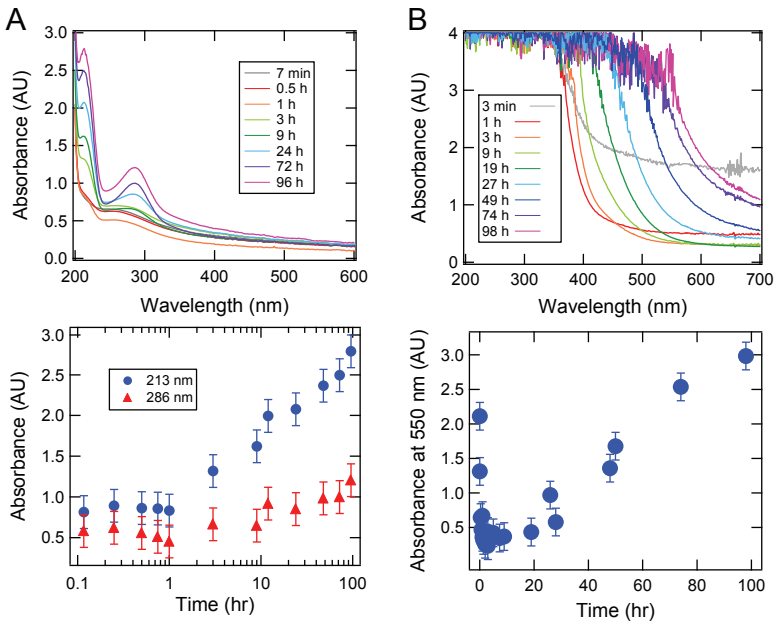

Fig. 4. Results of pendant drop tensiometry measurements of aqueous mixtures as a function of initial methylglyoxal concentration for aqueous solution, 3.1 M $(NH_4)_2SO_4$(aq), and 5.1 M NaCl(aq). The ratio of measured surface tension to the measured surface tension of Millipore water is shown. The measurements were made ≥24 h after mixing. Each point reflects the weighted average of five to eight measurements, and the error bars represent the standard deviation in the raw data. The best fit curve to each data set based on Eq. (2) is also shown.

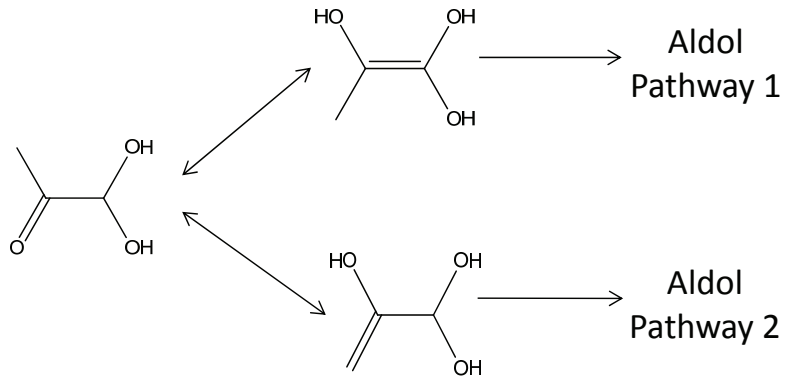

Scheme 1. Proposed reaction pathways for methylglyoxal.